

February 15, 1982

Self-pulsing and chaos in distributed feedback bistable optical devices

Herbert G. Winful
GTE Laboratories

Gene D. Cooperman
GTE Laboratories

Recommended Citation

Winful, Herbert G. and Cooperman, Gene D., "Self-pulsing and chaos in distributed feedback bistable optical devices" (1982). *Computer and Information Science Faculty Publications*. Paper 13. <http://hdl.handle.net/2047/d20000658>

Self-pulsing and chaos in distributed feedback bistable optical devices

Herbert G. Winful and Gene D. Cooperman

Advance Technology Laboratory, GTE Laboratories Incorporated, 40 Sylvan Road, Waltham, Massachusetts 02254

(Received 28 September 1981; accepted for publication 19 November 1981)

We show that the light transmitted by a nonlinear distributed feedback structure can be steady (time independent), periodic, or chaotic depending on the intensity of the input cw beam. The feasibility of an experimental demonstration of such behavior is discussed.

PACS numbers: 42.65.Bp, 42.80.Ks, 42.82.+n, 42.65.Cq

There has been much recent interest in optical systems whose transmission is a multivalued function of a control parameter such as the input intensity.¹ These bistable optical devices exhibit a rich variety of dynamic phenomena including hysteresis, discontinuous transitions, and self-pulsing instabilities. Ikeda *et al.* first pointed out that in the particular case of a ring cavity, the periodic self-pulsing solutions can bifurcate into a chaotic state in which the output intensity wanders randomly in time.² Such behavior was subsequently observed by Gibbs *et al.* who simulated the ring cavity by a hybrid electrical/optical device incorporating a delay line.³ It has been suggested³ that the chaotic behavior is a consequence of the fact that systems with delay in the feedback loop are described by difference equations which may possess instabilities in regions where the associated differential equations are stable. It is also considered an open question³ whether a standing-wave Fabry-Perot filled with a nonlinear index medium will exhibit self-pulsing and chaos.

In this letter we consider the dynamic behavior of a bistable distributed feedback structure whose steady-state properties were studied by Winful *et al.*⁴ Because the feedback mechanism is distributed continuously throughout the nonlinear medium, the system is accurately described by a set of partial differential equations instead of difference equations. The nonlinear distributed feedback structure is the optical analog of the Toda lattice⁵ (one-dimensional anharmonic mechanical lattice), and of the nonlinear electrical filter of Hirota and Suzuki.⁶ These latter structures support periodic pulse train solutions which are lattice solitons of the associated Korteweg de Vries equation. We find that the nonlinear optical distributed feedback structure also exhibits output pulsations when driven by a cw input. As the input intensity is increased, the output eventually becomes chaotic.

We consider a nonlinear medium with a periodic perturbation of its linear refractive index of the form [Fig. 1(a)]

$$n = n_0 + n_1 \cos 2\beta_0 z, \quad (1)$$

where $n_1 \ll n_0$. Such an index variation is achieved in practice by corrugating the surface of a waveguide or by introducing bulk periodic changes in the dielectric constant. The periodic structure serves as a reflection filter for light whose wavelength is close to the Bragg condition $\lambda \simeq \lambda_0 \equiv 2\pi n_0 / \beta_0$. Intensity-dependent refractive index changes are described by a nonlinear polarization

$$P^{NL} = n_0 \delta n(E) E / 2\pi, \quad (2)$$

where the index change δn satisfies a Debye relaxation

equation

$$\tau \frac{\partial \delta n}{\partial t} + \delta n = \frac{1}{2} n_2 |E|^2. \quad (3)$$

The nonlinear coefficient n_2 is related to the third-order susceptibility $\chi^{(3)}$. Such a model for material relaxation applies directly to Kerr media. It can also be derived from a two-level atomic model when the incident field is far off resonance. In that case the relaxation time τ is simply the longitudinal relaxation time T_1 . Expressions (1)–(3) characterize the material properties and can be substituted into Maxwell's wave equation

$$c^2 \frac{\partial^2 E}{\partial z^2} = \frac{\partial^2}{\partial t^2} [E + 4\pi(P + P^{NL})] \quad (4)$$

to solve for the field E . Here $P = (n^2 - 1)E / 4\pi$.

The field within the medium is taken as a sum of forward and backward propagating waves whose complex amplitudes are slowly varying functions of time and distance in the z direction:

$$E = E_F(z, t) e^{i(\beta z - \omega t)} + E_B(z, t) e^{-i(\beta z + \omega t)}. \quad (5)$$

Then combining Eqs. (1)–(5), applying the slowly varying envelope approximation and discarding terms with spa-

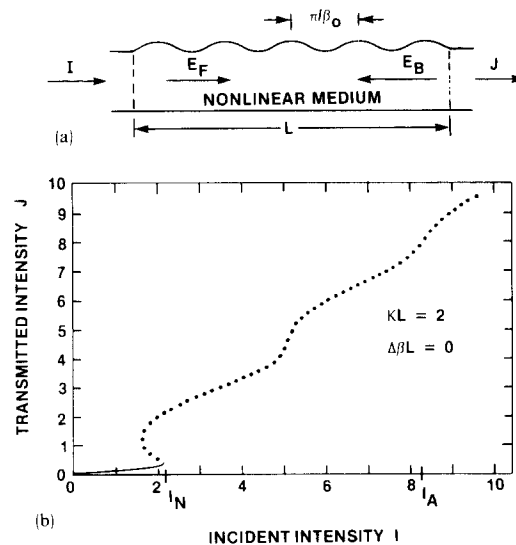


FIG. 1. (a) Schematic of a distributed feedback bistable optical device. The feedback is due to Bragg scattering from a surface corrugation (as shown) or from a bulk perturbation of the refractive index. (b) Steady-state transmitted intensity J vs incident intensity I for $\kappa L = 2$ and $\Delta\beta L = 0$. The solid line marks the stable solution. The dotted region is unstable, and the solution here is either periodic (for $I_N < I < I_A$) or chaotic ($I > I_A$).

tial variation faster than $e^{i2\beta z}$, we obtain the following set of coupled first-order equations:

$$\frac{\partial E_F}{\partial z} + \frac{n_0}{c} \frac{\partial E_F}{\partial t} = i\kappa E_B e^{-i2\Delta\beta z} + i\gamma(\delta n_0 E_F + \delta n_1 E_B), \quad (6a)$$

$$\frac{\partial E_B}{\partial z} - \frac{n_0}{c} \frac{\partial E_B}{\partial t} = -i\kappa E_F e^{i2\Delta\beta z} - i\gamma(\delta n_0 E_B + \delta n_1^* E_F), \quad (6b)$$

$$\tau \frac{\partial \delta n_0}{\partial t} + \delta n_0 = |E_F|^2 + |E_B|^2, \quad (6c)$$

$$\tau \frac{\partial \delta n_1}{\partial t} + \delta n_1 = E_F E_B^*, \quad (6d)$$

where $\kappa = \pi n_1 / \lambda_0$, $\gamma = \pi n_2 / \lambda$, and $\Delta\beta = \beta - \beta_0$. The coupling constant κ is a measure of the strength of feedback per unit length provided by the structure. The fields are subject to zero-reflection conditions at the boundaries of the grating.

In steady state ($\partial/\partial t = 0$) these equations reduce to the set discussed in Ref. 4 which can be solved analytically. The result for the case $\Delta\beta = 0$ is given by

$$I = \frac{J}{1 + (y_- / y_+) \operatorname{sn}^2[y_+ | (y_- / y_+)^2]}, \quad (7)$$

where I and J are the incident and transmitted intensities normalized by $|E_c|^2 = 2\lambda / 3\pi n_2 L$ and we define

$$y_{\pm} = \frac{1}{2} J \pm [(J/2)^2 + (\kappa L)^2]^{1/2}. \quad (8)$$

sn is a snoidal Jacobian elliptic function. This steady-state solution is shown in Fig. 1(b) where we plot the transmitted intensity versus incident intensity for a distributed feedback structure with a coupling constant $\kappa L = 2$.

The stability of the steady-state solution was investigated by solving the full time-dependent equations (Eqs. 6) numerically. The field equations were integrated along characteristics $\zeta = z - ct/n_0$ and $\eta = z + ct/n_0$, and the material equations were evaluated at discrete time steps using known field values from adjacent grid points. The grid size was halved repeatedly until convergence was achieved.

For step inputs of intensity less than the critical turn-on intensity I_n , the output settles down to the steady-state values indicated in Fig. 1(b) by the solid line. This positive slope region is thus stable in steady state. For step inputs just greater than I_n , the output consists of a steady train of pulses whose period is less than twice the round-trip time within the grating. As the input intensity is increased, the self-pulsation frequency also increases and the pulse widths grow smaller. Figures 2(a) and 2(b) show typical self-pulsing solutions for input intensities of 4 and 6 in our dimensionless units.

In these simulations, the material relaxation time was taken to be $\tau = T/20$, where T is the transit time ($T = n_0 L / c$) through the grating. As the relaxation time is increased, the pulse amplitudes diminish. Eventually the pulses are completely washed out when the relaxation time exceeds the transit time.

The pulsation frequency increases continuously with input intensity until at a certain critical intensity I_A the output becomes aperiodic. The transmitted intensity wanders in an apparently chaotic manner as a function of time. This behavior is shown in Fig. 2(c) where the input intensity was set at 9.

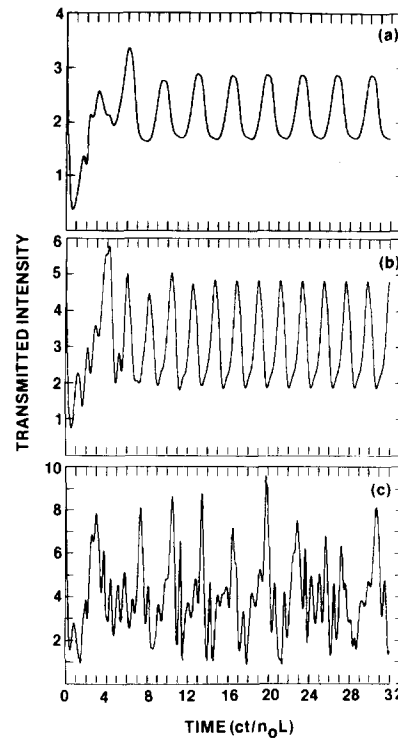


FIG. 2. (a) Self-pulsing solution for a step input of intensity 4. The material relaxation time is $\tau = 0.05$ in units of the transit time. (b) Self-pulsing solution for a step input of intensity 6. (c) Chaotic solution. Input intensity $I = 9$.

Physically one may understand the self-pulsing instability by considering the properties of a linear distributed feedback structure. For light whose wavelength lies in the stop band of the filter, the feedback provided by the structure is high and thus the cavity field is enhanced in the first few periods of the grating and drops off exponentially thereafter. For wavelengths outside the stop band, feedback is low, no enhancement of the field occurs, and the distribution is essentially uniform. Suppose now that one includes an intensity-dependent refractive index, and assume that at low input intensity the incident light wavelength lies within the stop band. Feedback is high, transmission is low, and the field builds up. As the input is increased, the high cavity field changes the refractive index of the grating, thus shifting the stop band. Eventually the structure is so detuned that the light wavelength no longer lies within the stop band. When this happens, feedback is reduced, transmission is high, and no field enhancement occurs within the cavity. This reduction of feedback and of cavity field causes the refractive index to relax back to its low value. The light wavelength now finds itself within the stop band, and the feedback increases once again. This process persists indefinitely, leading to a train of pulses.

The variable feedback situation that leads to self-pulsing may be simulated using a multiple mirror cavity of the type proposed by Szoke *et al.*⁷ and analyzed by Goldstone.⁸ Here the second cavity in a 3-mirror arrangement contains a nonlinear medium while the first cavity is empty and serves to provide the transit time and field enhancement effects needed for pulsing. The second cavity acts as a bistable re-

flector providing high reflection (feedback) at low input intensity and low reflection at high inputs.

The observation of effects described here requires nonlinear materials whose index change relaxes in a time short compared to the transit time of light through the grating. One solid-state nonlinear medium with a large nonlinearity ($n_2 \sim 1.8 \times 10^{-6} \text{ cm}^2/\text{MW}$)⁹ and subpicosecond response time is the polydiacetylene PTS (polytoluene sulphonate). For a 1-cm-long grating waveguide of PTS and a coupling constant $\kappa L = 2$, the intensity required for operation in the self-pulsing regime is on the order of $25 \text{ MW}/\text{cm}^2$. A quasi-cw source for this particular structure might be a Q-switched solid-state laser producing 20-ns pulses. The transmitted signal would then exhibit a substructure consisting of pulses whose widths are in the 10–100-ps range.

¹For a collection of papers on optical bistability, see *Proceedings on International Conference on Optical Bistability*, edited by C. M. Bowden, M. Cifitan, and H. R. Robl (Plenum, New York, 1981).

²K. Ikeda, H. Daido, and O. Akimoto, *Phys. Rev. Lett.* **45**, 709 (1980); K. Ikeda, *Opt. Commun.* **30**, 257 (1979).

³H. M. Gibbs, F. A. Hopf, D. L. Kaplan, and R. L. Shoemaker, *Phys. Rev. Lett.* **46**, 474 (1981).

⁴H. G. Winful, J. H. Marburger, and E. Garmire, *Appl. Phys. Lett.* **35**, 379 (1979).

⁵M. Toda, *J. Phys. Soc. Jpn.* **23**, 501 (1967). A general discussion of nonlinear lattice equations is contained in A. C. Scott, F. Y. F. Chu, and D. W. McLaughlin, *Proc. IEEE* **61**, 1443 (1973).

⁶R. Hirota and K. Suzuki, *Proc. IEEE* **61**, 1483 (1973).

⁷A. Szoke, V. Daneu, J. Goldhar, and N. A. Kurnit, *Appl. Phys. Lett.* **15**, 376 (1969).

⁸J. Goldstone and E. Garmire, *IEEE J. Quantum Electron.* **QE-17**, 366 (1981).

⁹J.-P. Herman and P. W. Smith, presented at the 11th Int. Quantum Electron. Conf., Boston, MA, June 1980.

Electron beam pumped cw Hg ion laser

J. J. Rocca,^{a)} J. D. Meyer, and G. J. Collins^{b)}

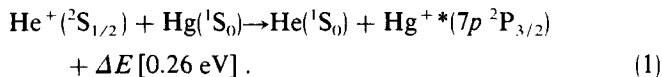
Department of Electrical Engineering, Colorado State University, Fort Collins, Colorado 80523

(Received 5 November 1981; accepted for publication 23 November 1981)

We have obtained cw laser action using electron beam excitation of a He-Hg mixture. This represents a new method of exciting cw lasers and offers the possibility of increased efficiency for ion lasers.

PACS numbers: 42.55.Hq, 42.60.By

We have obtained cw laser radiation on the 6149.9-Å line of the Hg^+ ($\text{HgII}: 7p^2P_{3/2}^0 \rightarrow 7s^2S_{1/2}$) by exciting a He-Hg gas mixture with a dc electron beam. This is the first time that a cw ion laser has been obtained using electron beam excitation. The dominant excitation mechanism is proposed to be charge transfer excitation of the $\text{HgII } 7p^2P_{3/2}^0$ from the $\text{HeII } ^2S_{1/2}$ according to the reaction¹



The conventional manner of exciting cw ion lasers is to use electron collisions in the positive column region of a discharge.²⁻⁴ A positive column has roughly a Maxwellian electron energy distribution with a mean electron energy of 3 to 8 eV, depending on pressure, current density, bore diameter, and magnetic field strength.^{2,4} However, the ionization and excitation cross sections of many upper laser levels peak above 100 eV.^{5,6} Hence, only those energetic electrons in the tail of the Maxwell-Boltzmann energy distribution are energetic enough to provide direct excitation. As a consequence very large current densities (hundreds of A/cm^2) are generally required to excite noble gas ion lasers, resulting in laser operating efficiencies of 5×10^{-4} . In the case of metal vapor

ion lasers, the metal impurity, when added to the discharge, drastically lowers the electron temperature of the positive column plasma.⁷ As a result, the metal vapor concentration and the electron temperature cannot be independently optimized. The electron energy characteristics of the positive column become even more undesirable for UV and VUV ion lasers where the upper laser levels are in multiply ionized species.⁸ The laser operating efficiencies for Ar^{++} and Kr^{++} lasers, for example, are typically 10^{-4} . We believe that electron beam pumped ion lasers have the potential advantage of increased efficiency as well as the generation of cw radiation in the VUV region because of the large density of energetic electrons. Hollow cathode ion lasers⁹ have an electron beam component in the electron distribution, but it is small and inefficiently produced. The beam component accounts for typically only 10% of the total discharge cur-

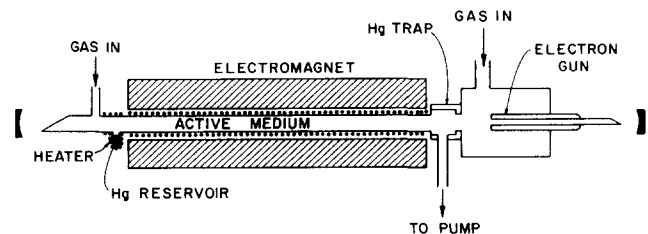


FIG. 1. Schematic diagram of electron beam excited laser apparatus.

^{a)}Spectra-Physics Industrial Fellow.

^{b)}Alfred Sloan Fellow, 1979-81.